Field Guides

Critical zone evolution: Climate and exhumation in the Colorado Front Range

Suzanne P. Anderson, Robert S. Anderson, Gregory E. Tucker and David P. Dethier

Field Guides 2013;33;1-18
doi: 10.1130/2013.0033(01)

The Geological Society of America
Field Guide 33
2013

Critical zone evolution: Climate and exhumation in the Colorado Front Range

Suzanne P. Anderson
Institute of Arctic and Alpine Research (INSTAAR) and Department of Geography, University of Colorado, Boulder, Colorado 80309, USA

Robert S. Anderson
Institute of Arctic and Alpine Research (INSTAAR) and Department of Geological Sciences, University of Colorado, Boulder, Colorado 80309, USA

Gregory E. Tucker
Cooperative Institute for Research in Environmental Sciences (CIRES) and Department of Geological Sciences, University of Colorado, Boulder, Colorado 80309, USA

David P. Dethier
Geosciences Department, Williams College, Williamstown, Massachusetts 01267, USA

ABSTRACT

The architecture of the critical zone—the distribution of mobile regolith, the thickness of weathered rock, and their characteristics, as well as the topography of the land surface—is shaped by erosion and weathering processes that depend upon both lithology and climate. In this trip we explore the Boulder Creek watershed, a landscape that juxtaposes uplifted Precambrian crystalline rocks of Colorado's Front Range against Mesozoic marine sedimentary rocks underpinning the western edge of the High Plains. The landscape is strongly shaped by Quaternary climate cycles operating on this template inherited from the Laramide orogeny. Stop 1 will provide an overview of the abrupt topographic step at the Front Range–High Plains join, where we will discuss fluvial strath terraces on the Plains. At Stop 2 in Betasso Preserve, we will discuss the impact of the canyon cutting set off by late Cenozoic exhumation of the High Plains on the hillslopes and groundwater systems lining the master stream. At Stop 3, we will hike 2 miles down Gordon Gulch, a focus site in the Boulder Creek Critical Zone Observatory. At stops on the hike, we will discuss exhumation rates, climate-modulated weathering, hillslope hydrology and hillslope sediment transport, and the influence of slope aspect on these processes. Our goal is to focus on the history of climate-driven erosion and weathering processes, and how to incorporate these processes into quantitative models of landscape evolution.

Anderson, S.P., Anderson, R.S., Tucker, G.E., and Dethier, D.P., 2013, Critical zone evolution: Climate and exhumation in the Colorado Front Range, *in* Abbott, L.D., and Hancock, G.S., eds., Classic Concepts and New Directions: Exploring 125 Years of GSA Discoveries in the Rocky Mountain Region: Geological Society of America Field Guide 33, p. 1–18, doi:10.1130/2013.0033(01). For permission to copy, contact editing@geosociety.org.

INTRODUCTION

The Front Range is one of a number of mountain ranges formed in the compressional tectonics of the Tertiary Laramide orogeny (e.g., Bird, 1988, 1998; Dickinson et al., 1988). At this location, starting at roughly 65 Ma, the orogeny thrust Paleoproterozoic crystalline rocks up against the marine sediments from the Cretaceous Western Interior Seaway. The first-order topographic feature of the watershed arises from this lithologic contrast set by tectonic history: the crystalline rocks of the Front Range tower above the soft sedimentary rocks of the Plains, separated by an abrupt topographic front. As the name suggests, the Plains comprise smooth topography with broad fluvial terraces standing in low relief above the modern rivers. The Front Range is characterized by more rugged terrain cut into crystalline rocks, notably deep canyons gashed upvalley from the Plains, and steep-sided glacial valleys hugging the range crest (see R.S. Anderson et al., 2006; S.P. Anderson et al., 2012).

The canyons cut along the eastern edge of the Front Range reflect an acceleration in regional erosion, including erosion of the proximal part of the Denver Basin, beginning in the Pliocene (Fig. 1). During this time, east of the Front Range, the South Platte River and its tributaries cut through the Miocene Ogallala Group sediments, as well as older Tertiary sediments (Fig. 2).

The headwaters of Boulder Creek were glaciated during the Pleistocene (Fig. 3), which is manifested in U-shaped valleys and areas of bare, abraded bedrock surfaces in the valley floors and walls. Below the glacier limit is the Rocky Mountain Surface, a region of relatively low relief mantled by thin soils and dotted with tors (outcrops). This area is a product of weathering and erosion since the end of the last phase of uplift in the Laramide orogeny. At its outer, eastern margin, the Rocky Mountain Surface is dissected by river canyons, each with a prominent knickpoint or knick zone at its head (R.S. Anderson et al., 2006). Hillslopes lining the canyons are stripped of weathering profiles, although the mechanism is base-level lowering rather than glacial abrasion (Fig. 3). Hillslopes are steepest and show the least weathering in the knick zone, and become progressively less steep and more weathered with distance downstream from the knick zone, a progression that reflects the evolution of the critical zone following the perturbation of rapid river incision. Finally, on the Plains, topography reflects a bimodal erosion history, in which the rivers either broaden their footprint by lateral planation, or cut into bedrock and abandon the alluvium-mantled strath terraces (see Fig. 3). The long periods of lateral planation, punctuated by periods of fluvial incision on the Plains (Dühnforth et al., 2012), are coincident with aggradation and removal of fluvial fill terraces in the canyons. Headward progress of the knick zone up the canyon accelerates when canyon fill terraces are removed, and decelerates when fill aggrades.

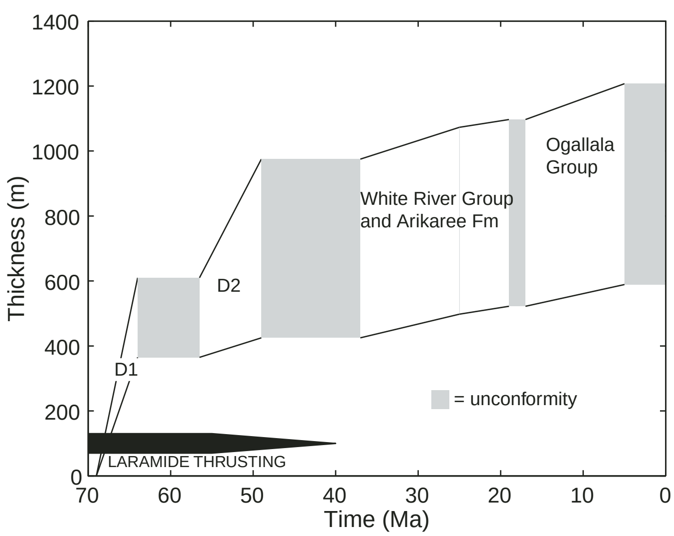

Figure 1. Schematic illustration showing depositional (white) and erosional (gray) episodes in the central and northern Colorado Piedmont during the Cenozoic. Figure is based on preserved sedimentary record in the Denver Basin (Late Cretaceous to early Tertiary) and Colorado-Wyoming border region (mid-late Tertiary). Note that this composite illustration combines synorogenic sequences D1 and D2 from the Denver Basin (Raynolds, 2002) with mid- to late-Tertiary units in northeastern Colorado (based on map by Courtright and Braddock, 1989) (from Tucker and van der Beek, 2012).

Understanding how erosion and weathering together shape the architecture of the critical zone forms the core question of the Boulder Creek Critical Zone Observatory (S.P. Anderson et al., 2008). The question unites exploration of topographic signatures of erosion, understanding distributions of surface features such as soil, outcrops, and vegetation, and deciphering the subsurface reach of weathering and movement of water. In each of the varied erosional settings of the Front Range and adjacent Plains, the architecture of the critical zone represents the integrated effects of weathering front propagation and erosional exhumation over time operating on the particular rocks with their particular tectonic histories as they are brought to the surface by exhumation. In the alpine regions of the Front Range, rapid erosion and low chemical weathering front propagation rates under glaciers explains the truncated weathered profiles. Soils in the alpine areas are found only on deposits, rather than from in situ weathering of the bedrock. For instance, moraines, glacial till, talus and colluvial slopes, and very old diamicton (poorly sorted sediment of unspecified origin) on the ridge tops above recent glacial limits are deposits in which weathering processes produce soils on preexisting sediments, augmented by eolian inputs (Muhs and Benedict, 2006). The deepest weathering profiles are found on the Rocky Mountain Surface, where, although spatially variable, they average 7 m in depth (Dethier and Lazarus, 2006). In contrast, on hillslopes lining the fluvial canyons, bare rock slopes dominate. Slope angles, extent of mobile regolith cover, and rock weathering vary owing to differences in time since perturbation by fluvial incision. The weathered profile is thinnest and least developed along the river channel and near the knick zone, places where the erosion rates exceed weathering front propagation rates. One can assess development of the critical zone in

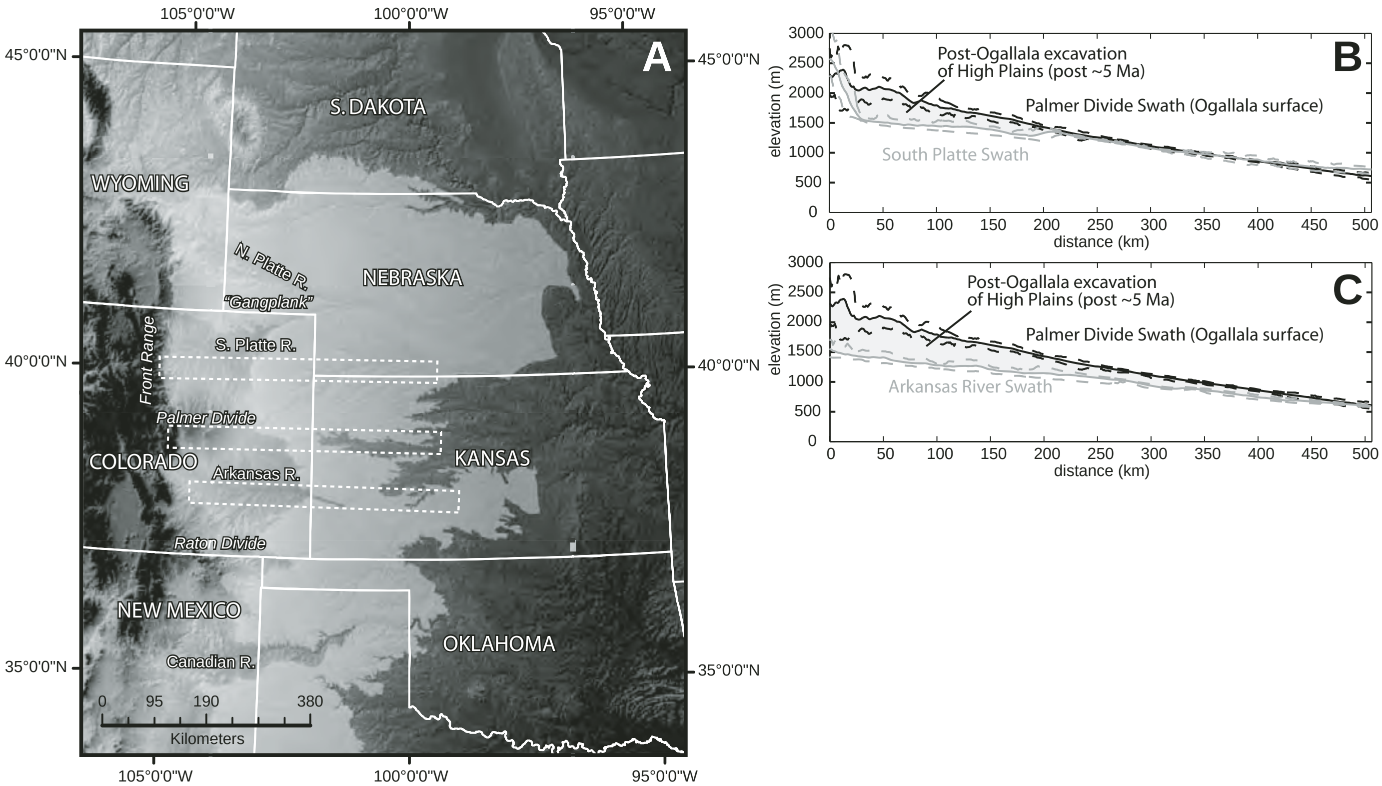

Figure 2. Incision of the North American High Plains. (A) Map extent of remaining Ogallala Group (light-gray shading) shows planview patterns of incision into this surface. Thin dashed boxes show extent of swath profiles for South Platte and Arkansas Rivers, which are compared with the swath profile from the Palmer Divide in B and C. (B and C) Swath profiles show vertical patterns of incision driven by the Arkansas and South Platte rivers, relative to the Palmer Divide interfluve. Solid lines show average elevation as a function of distance within each swath; dashed lines show minimum and maximum elevations. Note that the South Platte swath is oblique to the course of the river; orientation was chosen to run downdip along the Ogallala surface (after Wobus et al., 2010).

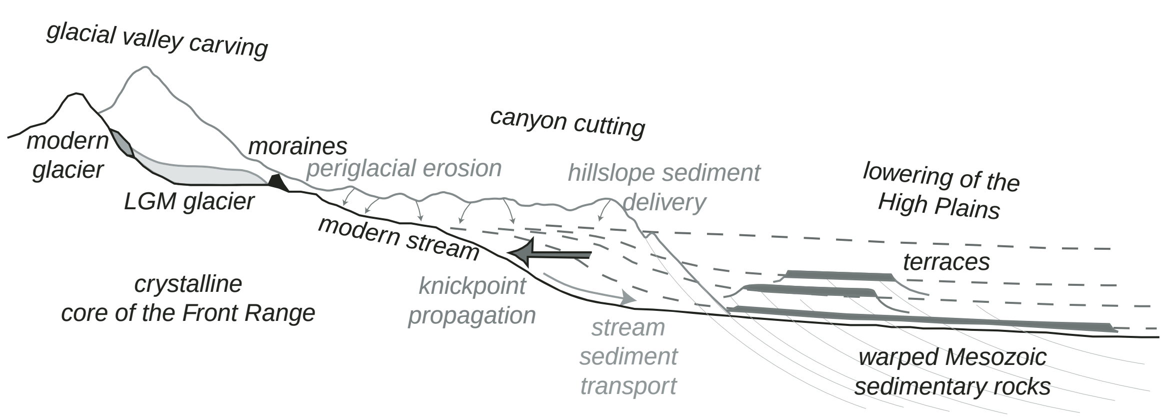

Figure 3. Schematic cross-section from the headwater divide of Colorado Front Range to the western edge of the High Plains illustrating how water and sediment transfers affect erosion in distant regions. Three distinctive erosion regimes exist along the cross-section: glacial valley carving in the headwaters, canyon cutting within the Range, and fluvial lowering of the High Plains. These result from the actions of glaciers, hillslope sediment transport systems, and rivers. During glacial periods, glaciers carved the headwaters and periglacial slope processes delivered sediment to the streams outside the glacial limit (small arrows). Fluvial downcutting is favored during deep interglacials when the sediment supply from upstream declines. The locus of downcutting begins in the soft sedimentary rocks on the Plains. A knickpoint propagates upstream (large arrow) into the hard crystalline rock upstream, carving canyons in the Front Range. (After S.P. Anderson et al., 2012, fig. 4.)

any of these locations as a one-dimensional problem of weathering processes generating the critical zone, and erosion removing material from the critical zone. Because rates of river incision respond to sediment flux, the production and transport of sediment upstream can influence process rates downstream.

STOP 1: NCAR TABLE MESA LABORATORY PARKING LOT

The eastern edge of the Front Range is abrupt, forming the scenic backdrop to the Denver metropolitan area. This results from the juxtaposition of easily eroded rocks of the High Plains (largely Cretaceous shales) against Precambrian crystalline rocks of the core of the Front Range. The topographic step and the change from smooth to rugged local relief at the mountain front reflect not active faulting, but a difference in the erodibility of the rocks.

A short walk downhill from the parking lot of the National Center for Atmospheric Research (NCAR) laboratory, built in the 1960s to the design of I.M. Pei, provides a view of the prominent fluvial strath terraces cut into the soft bedrock of the Plains by rivers draining the Front Range (Fig. 4). To the south, the most extensive and oldest of these is the Rocky Flats surface, now host to the large wind turbines being tested at the National Renewable Energy Laboratory (NREL) facility seen on the horizon. Between the Rocky Flats surface and the viewpoint runs South Boulder Creek, which is bounded by several lower, younger surfaces. Each of these surfaces consists of a beveled bedrock terrace (strath terrace) etched across Laramide-warped Cretaceous rocks, and capped with several meters of alluvial gravel sourced from the crystalline rocks of the range. At the viewpoint itself, locally sourced sedimentary rocks, comprised of sediments shed from the Ancestral Rockies, cap the surface. These sedimentary units, including the Pennsylvanian-age Fountain Formation, were uplifted and tilted in the Laramide orogeny and subsequently exhumed to create the Flatirons that form the dramatic backdrop to the NCAR site and the city of Boulder.

The terraces have long been mapped (e.g., Scott, 1960, 1962; Madole, 1991; Cole and Braddock, 2009), and are given names reflecting correlations based largely upon height above the adjacent streams and degree of soil development (Fig. 5). Dating of these surfaces can constrain long-term exhumation of the edge of the Plains. Recent research employing cosmogenic radionuclides ^{10}Be and ^{26}Al has revealed comparatively young ages of several of these surfaces (Riihimaki et al., 2006; Dühnforth et al., 2012). These ages, best interpreted as the timing of last deposition on the surface, support a conceptual model of the formation of strath terraces in which sediment supply governs switching between lateral widening of valley walls and vertical incision of channel floors (Hancock and Anderson, 2002). The widths and times of last deposition on these surfaces suggest that they are occupied and widened for long periods of time corresponding to glacial climates, and are abandoned in rapid pulses of vertical incision into the Cretaceous shale during deep interglacials. As these surfaces occur at the outlets of both drainage basins that drain the glaciated crest and those that do not access the glaciated crest (green and red channels in Fig. 5, respectively), access to glacially derived sediment is not required. We hypothesize that modulation of the sediment supply from nonglaciated basins is also slaved to climate, as the landscape becomes more productive of sediment when periglacial processes reign during glacial times. Rates of incision into the Cretaceous Pierre Shale on the Plains during times of very low sediment supply appear to exceed 1 mm/yr (Dühnforth et al., 2012). This argument suggests a strong role for critical zone processes in governing the topographic form of the western edge of the High Plains.

Key Points at Stop 1

- The Laramide orogeny juxtaposed hard crystalline rocks against soft sedimentary rocks, setting up the framework of bedrock with contrasting erodibility in the present landscape.
- Alluvium-mantled, fluvial strath terraces record exhumation on the Plains during the Quaternary. While onset of exhumation is not well established, cosmogenic dating of these surfaces constrains the pace of incision in the past few hundred thousand years.
- The terraces appear to be occupied and widened during glacial periods and abandoned due to vertical channel incision during deep interglacials.

STOP 2: BETASSO PRESERVE

Betasso Preserve, part of the Boulder County Parks and Open Space system, includes areas of rolling terrain of the Rocky Mountain Surface and steep slopes slaved to the incision of Boulder Creek. Within the crystalline rocks of the Front Range, exhumation takes the form of canyon cutting, rather than terrace planation and abandonment seen at Stop 1 on the Plains (Fig. 3). Each river draining eastward in the Front Range has a knickpoint or knick zone indicating the headward progress of exhumation. The steep bedrock walls lining the canyons at knick zones give way to shallower slopes with varying degrees of mobile regolith cover with increasing distance downstream (Fig. 6). Boulder Creek Critical Zone Observatory selected a steep watershed within Betasso Preserve for monitoring to represent areas that have undergone transient erosion in response to base-level lowering (S.P. Anderson et al., 2008). The informally named ephemeral Betasso creek discharges into Boulder Creek ~7.5 km downstream from the knick zone. The watershed therefore represents the state of evolution several million years after initial rapid base-level lowering associated with passage of the knick zone in Boulder Creek, assuming knickpoint celerity of 2.5–5 mm/yr. Base level for this watershed, set by Boulder Creek, has probably varied over time due to alluviation and scour over glacial-interglacial cycles, and possibly due to multiple waves of incision from lowering on the Plains.

Figure 4. View looking south from Stop 1, along the short trail running east from the parking lot at the National Center for Atmospheric Research. Eastern edge of High Plains is punctuated by smooth, low-sloping surfaces, as in Rocky Flats on the left horizon. Local rivers cut into the Cretaceous shales leave a series of terraces bounding them. South Boulder Creek lies in the middle ground, bounded by at least two other surfaces below Rocky Flats. The surface on which NCAR is built is being eroded from the east by hillslope and small gully systems, exposing coarse clasts in the foreground that mantle the strath surface (photo by R.S. Anderson).

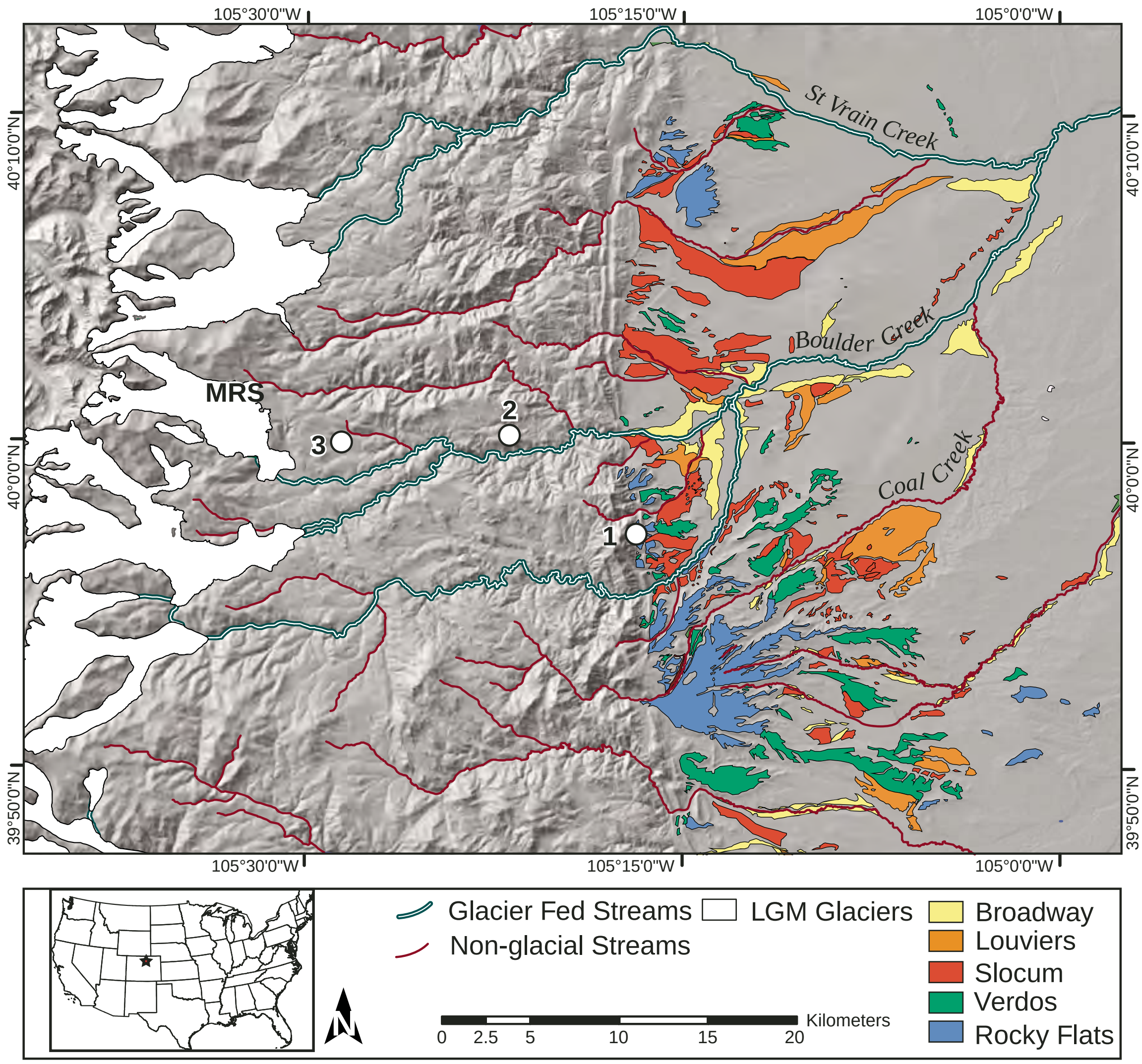

Figure 5. Shaded relief image of the Colorado Front Range near Boulder showing glacier extent at the Last Glacial Maximum (LGM) and the locations of Pleistocene fluvial strath terraces. Locations of field trip Stops 1–3 are shown with white circles, as well as our lunch stop at the Mountain Research Station (MRS). The fluvial strath terraces step down from the highest Rocky Flats to the lowest Broadway terrace (Madole, 1991). The strath terraces record exhumation of the Plains as the rivers have cut downwards, and are found lining both glacier-fed and non–glacier-fed rivers. The glacier-fed river systems shown here are South St. Vrain Creek (to the north) and Boulder Creek (to the south), which join on the Plains. Glacier extents from Madole et al. (1998), terraces from Cole and Braddock (2009), after Scott (1962, 1963) (modified from Dühnforth et al., 2012, fig. 5, and S.P. Anderson et al., 2012, fig. 5).

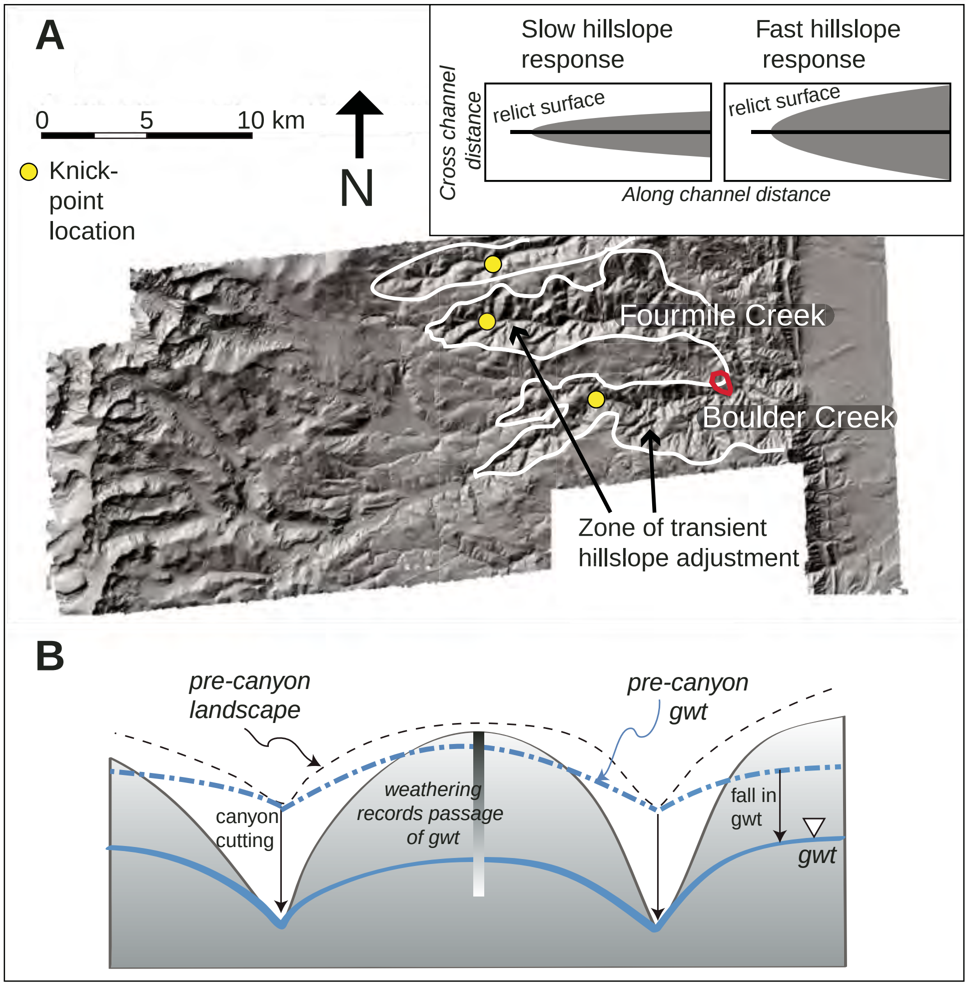

Figure 6. (A) Light detection and ranging–derived shaded relief map of Colorado Front Range along Boulder Creek. Approximate locations of knick zones are shown with yellow circles, and areas of transient hillslope response to canyon cutting are outlined in white. Betasso catchment, circled in red, straddles the apparent boundary between the relict area of low relief and the zone of transient adjustment. Inset shows hillslope response to channel incision under differing transport efficiencies, based on figure 11 in Mudd and Furbish (2007). (B) Schematic cross section illustrating the hillslope and groundwater table (gwt) response to canyon cutting. Dashed lines represent pre-canyon cutting conditions, and solid lines represent the present conditions (after S.P. Anderson et al., 2012, fig. 7).

Just above its confluence with Boulder Creek, Betasso catchment is steep and flanked by steep slopes (Fig. 7). Bedrock outcrops in the lower catchment are visible on the light detection and ranging (LiDAR)–derived shaded relief map, especially on the western slopes. In the bowl-shaped upper catchment, however, a colluvial fill that in places exceeds 4 m in thickness can be discerned from the smooth topography etched with several deep gullies. Bedrock ribs are again visible around the upper catchment divide. We will examine only one weathered profile in the watershed, in a location near the catchment divide and above the thick colluvium. The impression given by patterns of weathering, the topography, and the distribution of colluvium in the catchment is that base-level lowering has impacted the lower catchment but has had little influence on the upper catchment.

A borrow pit located at the top of the Betasso Link bike trail, near its intersection with Betasso Road (the access to the City of Boulder water filtration plant), provides an exposure of a weathered profile near the top of the watershed in the low-relief surface. The profile comprises a 15–30-cm-thick layer of mobile regolith over several meters of saprolite (Fig. 8) developed in the early Proterozoic Boulder Creek granodiorite (Gable, 1980). The presence of highly erodible saprolite at this location shows that hillslope adjustment associated with the base-level lowering along Boulder Creek has not propagated all the way to the catchment divide.

The profile shows minor enrichments in kaolinite and Fe-oxides in the top 50 cm, and a far greater enrichment in smectite (Fig. 8). Smectite and Fe-oxides are found in hydrothermally altered bedrock throughout the Boulder Creek batholith (Dethier and Bove, 2011). However, the lack of Fe-oxides below ~50 cm depth, and the strong bulge in smectite concentrations at the top of the saprolite suggests that in this profile these are neoformed minerals due to weathering of the bedrock. The smectite bulge coincides with a drop in plagioclase concentration, further supporting this interpretation. However, several lines of evidence suggest that more is going on here. First, the Fe-oxides are dominated by magnetite, a primary mineral in the granodiorite parent rock. Second, the large amount of smectite throughout the profile is unusual, and more than is easily explained by pedogenesis alone. Clay fills microfractures in quartz and plagioclase grains in thin sections from the profile, even at 150 cm depth (Fig. 9). The drop in plagioclase is associated with a change in parent material lithology suggested by a change in Ca/Na ratios in bulk samples (not shown).

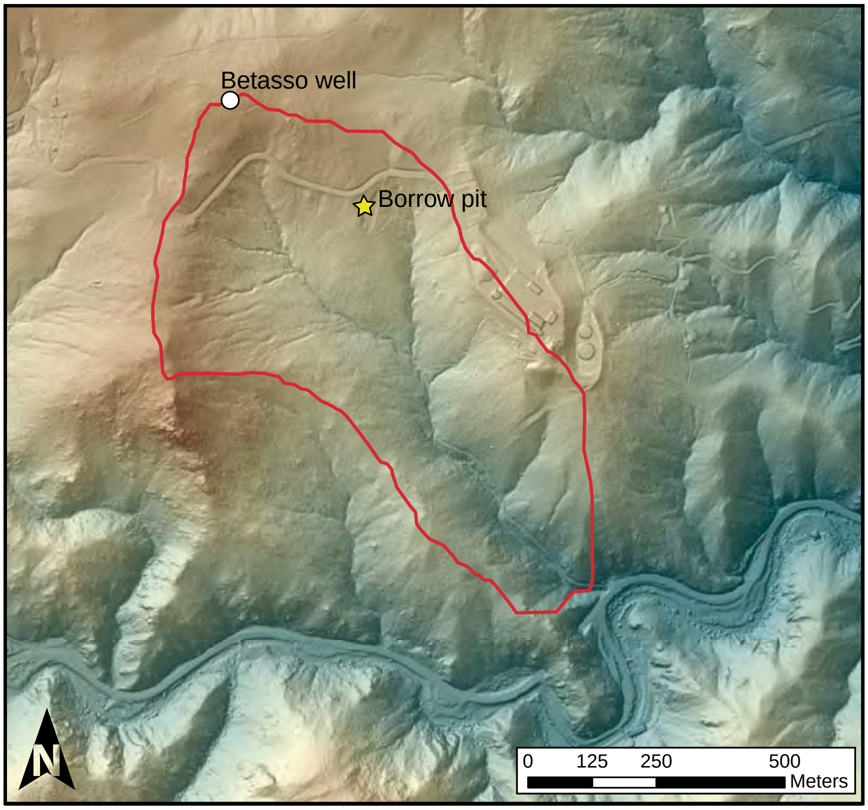

Figure 7. Shaded relief map of Betasso catchment in Betasso Preserve, showing locations of borrow pit and groundwater well resulting from "drill the ridge" campaign.

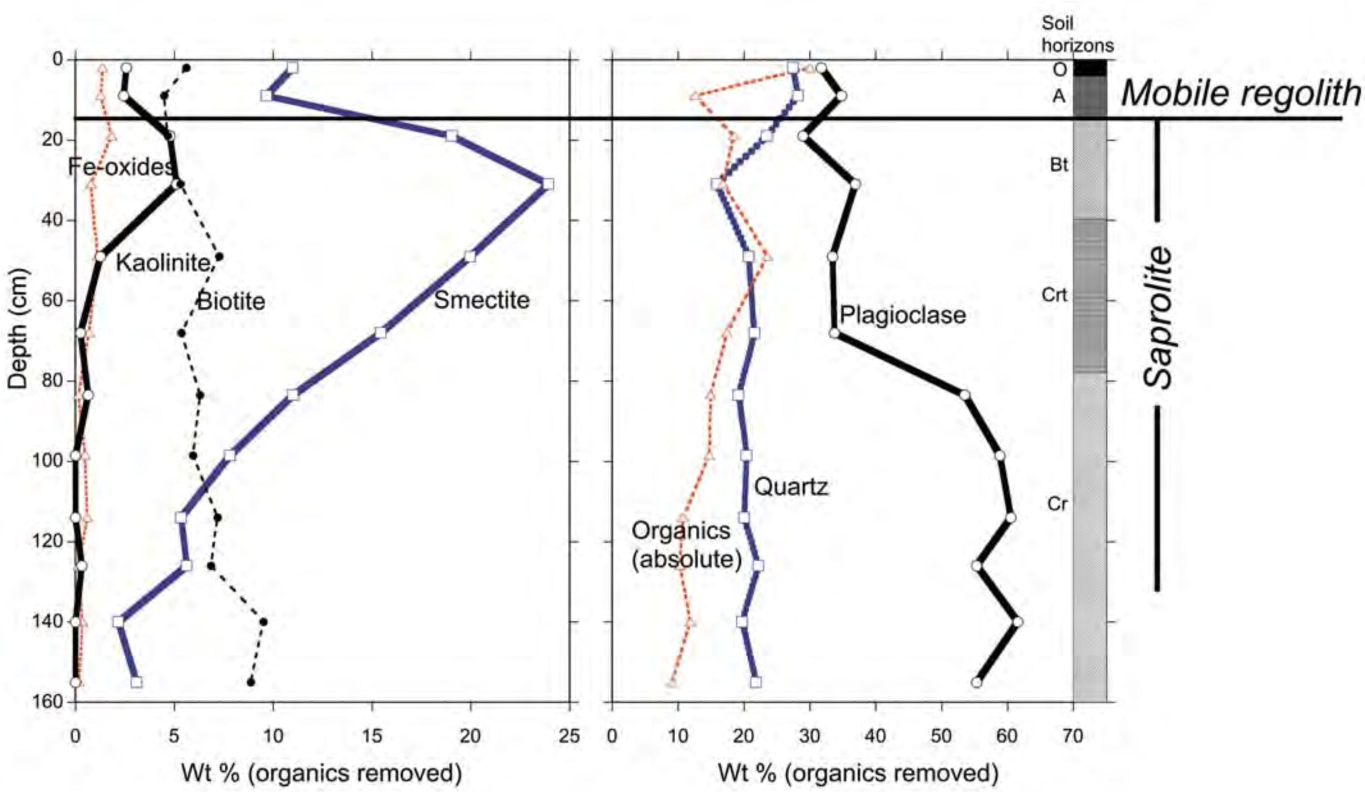

Figure 8. Mineralogy from borrow pit at top of Betasso catchment. Samples analyzed using quantitative X-ray diffraction (XRD) technique of Środoń et al. (2001). Note the difference in *x*-axis scale for the two panels. All phases except "organics" have been normalized to remove the organic contribution. Soil horizons based on field observations and these mineralogical findings. *Mobile regolith* is material that is detached from bedrock and free to move on slope; *saprolite* is weathered in place, and contains original rock structure. Soil developed on Boulder Creek granodiorite (Gable, 1980). Data courtesy of Alex E. Blum, U.S. Geological Survey.

These features may arise from eolian inputs of smectite-rich material, or from a layer of hydrothermally altered parent material. The domination of smectite over kaolinite in the clay phases suggests that leaching of cations is incomplete, as one might expect in the semi-arid climate of the Front Range.

Monitoring of soil moisture in saprolite at two sites in the Betasso watershed reveals that saprolite below about half a meter in depth tends to stay relatively dry (below 5% volumetric water content) throughout the year. One of these sites is at the borrow pit exposure (Fig. 10). During 2011, the deeper saprolite moisture sensors responded to late spring snow (April), early summer rain, and to October rains, but did not respond to other events during the year. These data support the hypothesis that the availability of water limits the rate of chemical weathering in saprolite in this semi-arid environment.

Understanding the deep flow system and full weathered profile were targets of a project to drill the ridge at Betasso in January 2013. Situated at the drainage divide above the borrow pit, drilling reached 124 m (406 ft). Core was recovered over about half of the borehole, primarily the top of the boring (Fig. 11). Extensive sections were air-hammered without core recovery owing to friable rock, apparently due to hydrothermal alteration of the granodiorite. The fracture density increased dramatically just above the first air-hammered section at ~53 m (175 ft). The completed well is 121 m deep (398 ft), due to debris filling in the bottom 3 m (8 ft). It is cased to a depth of 60 m (198 ft), and screened from 60 to 121 m (198–398 ft). During drilling, a prominent fracture encountered at 43 m (143 ft) was flagged as possibly water filled based on dramatic drop in the rate of loss of drilling water during drilling, although no water was detected in the borehole after sitting overnight. Water inflow at a low rate (estimated ~1.9 L/min, or ~0.5 gal/min) was detected at 101 m (331 ft), which caused the water level in the borehole to rise 17 m (56 ft) overnight. In the months since drilling was completed, the water level measured manually in the well has hovered around 29 m (95 ft) depth, and rose to 28 m (91.6 ft) following heavy snows in April. An automated water-level sensor was installed in May 2013.

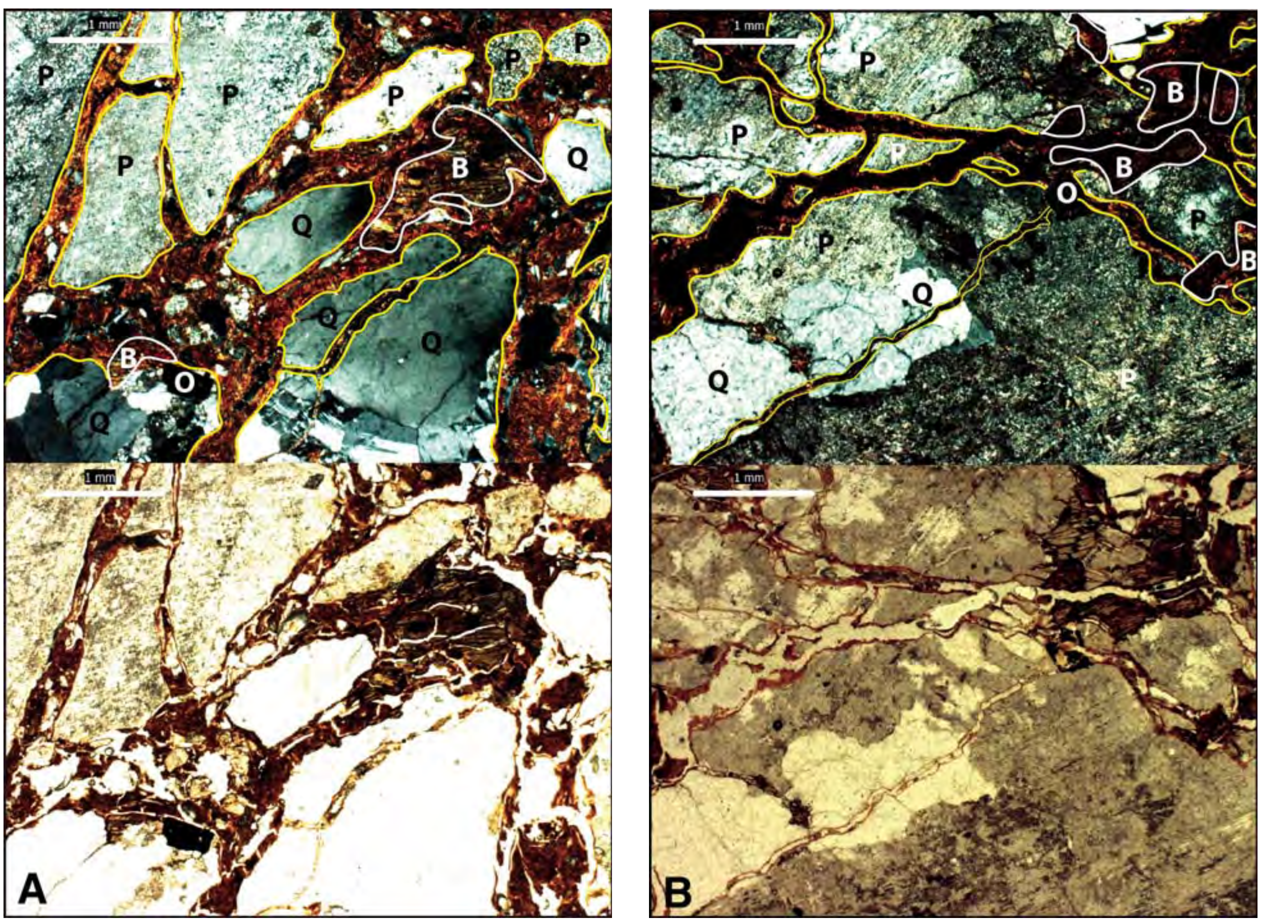

Figure 9. Thin sections from 50 cm and 150 cm in profile shown in Figure 7. Bottom half in transmitted light, top half in cross-polarized light. P—plagioclase, Q—quartz, B—biotite, O—opaque. Note clay groundmass in fractures in quartz grains in particular, at both depths.

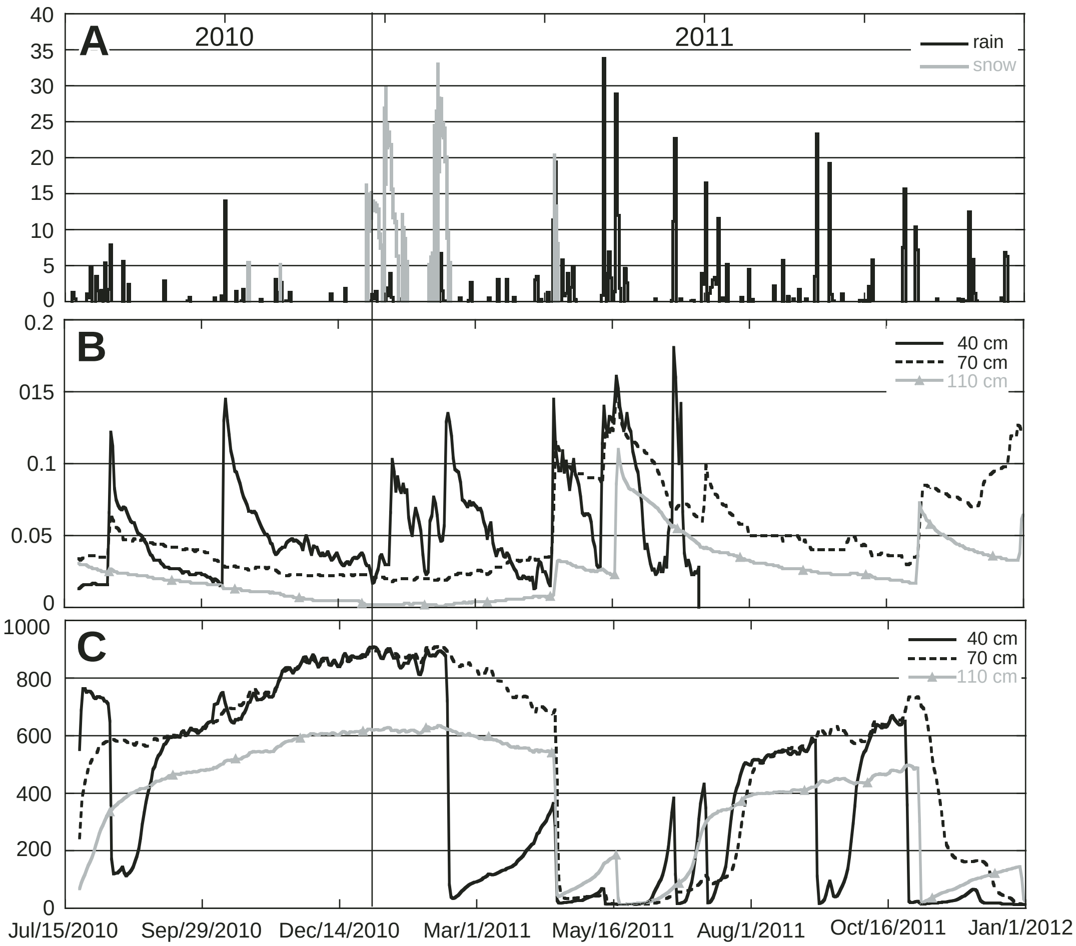

Figure 10. Precipitation, soil moisture, and matric potential in saprolite at the Betasso Borrow Pit site (from A.L. Langston, 2013, personal commun.).

In addition to providing data on deep-water dynamics, the core and samples collected during air hammering will be used to analyze alteration products, fractures, and rock characteristics. We hypothesize that the vertical pattern of rock alteration from the borehole may reveal evidence of dropping of base level associated with incision of Boulder canyon (Fig. 6B).

Key Points at Stop 2

- The 1.7 Ga granitic rocks of the Boulder Creek batholith exposed here are weathered to soil and saprolite. In places, local hydrothermal fluids, probably during and after the Laramide orogeny, altered rock at depths well below the top-down weathering profile.
- The strong soil here is smectite-rich, suggesting both incomplete leaching and additions to the soil, perhaps from eolian activity.
- Hydrologic monitoring suggests that the saprolite below a depth of 0.5 m remains dry most of the time and that the water table is >28 m below the surface at the divide.
- Extensive areas of soft saprolite and local colluvium >4 m thick in the upper watershed show that base-level lowering associated with deepening of Boulder Canyon has not strongly impacted the upper part of the Betasso catchment.

DRIVE UP BOULDER CANYON BETWEEN STOPS 2 AND 3

Between Stops 2 and 3, we drive up Boulder Canyon. In the lowermost canyon, the canyon walls are steep and rocky. Block sizes and outcrop patterns are governed largely by fracture patterns that reflect the Laramide stress field through which these crystalline rocks moved tens of millions of years ago. Trees pry blocks off the hillslopes by root growth in cracks (Fig. 12). We drive past Boulder Falls, a discrete knickpoint in North Boulder Creek near its confluence with Middle Boulder Creek. The road follows Middle Boulder Creek. For the next few kilometers upstream, the creek remains very steep (signs advise drivers going downhill of 10% grades), and the rocky walls are steepest, providing many rock-climbing challenges. A few kilometers

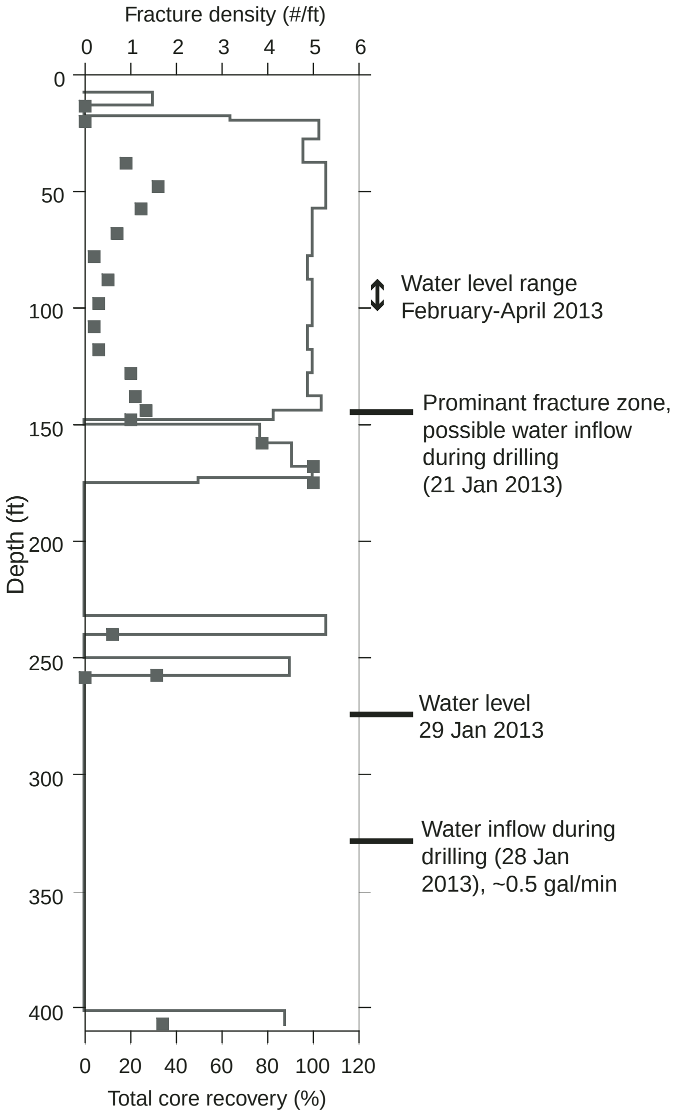

Figure 11. Log from core drilling at the ridge top in Betasso in January 2013. Plot shows fracture density in drilling runs (data points), core recovery (stepped line), and notes on water during drilling and in the first months following drilling.

above the confluence of Middle and North Boulder Creeks, the slope of the river declines, and the valley walls relax to much less rocky tree-cloaked hillslopes. We have passed through the knick zone of Boulder Creek, which represents the position in the landscape upstream of which the stream and hence the adjacent landscape has not "felt" the exhumation of the High Plains (Fig. 6A).

A few fluvial fill terrace remnants, rare fluvial strath terrace remnants, and isolated bedrock potholes are found within Boulder Canyon, most ~7–10 m above the present channel. These are dated to 12–20 ka based on ^{10}Be exposure ages (Schildgen et al., 2002), and they record aggradation and degradation of alluvial fill terraces within the canyon during and immediately following the end of the last glaciation. These erosional and depositional features presumably record temporal variations in the production and exhumation of glacial sediment in the headwaters. Exhumation within the crystalline rock of the mountains differs in style and form from exhumation on the softer bedrock of the Plains. Rather than forming broad strath steps in the landscape, incision of rock by Boulder Creek is accomplished by a knick zone working its way upstream in the hard rock, casting off rock slopes that slowly recover following this passage (Fig. 6A). Downcutting in both environments appears to be associated with interglacial climates, when sediment supply declines; planation of straths on the Plains and aggradation of alluvium in the canyon occurs during glacial climates.

After passing Barker Meadow Dam, impounding Barker Reservoir, we obtain views of the crest of the Front Range. The Last Glacial Maximum (LGM) and earlier glaciers extended almost to the western edge of the town of Nederland on the west side of Barker Reservoir. The moraines there and in Green Lakes valley provide our best constraints on the timing of the maximum extents of the LGM and the penultimate glaciations (Schildgen, 2000; Schildgen et al., 2002).

For lunch, we will drive to the University of Colorado Mountain Research Station (MRS), which is situated on the Arapaho Moraine from glaciers in Green Lakes valley. The MRS is a research facility of the Institute of Arctic and Alpine Research devoted to advancement of study of mountain ecosystems. The MRS runs the Mountain Climate Program, which has measured meteorological data from four stations since 1952 (Pepin and Losleben, 2002).

STOP 3: GORDON GULCH WATERSHED

Starting from the drainage divide a few km east of the Peak-to-Peak highway, we will hike down the axis of the 2.7 km^2 Gordon Gulch drainage basin, exploring the evolution of hillslopes that bound the creek.

First, look west to see the summits of the Indian Peaks that grace the Continental Divide (Fig. 13). The valleys tuck little scraps of glaciers, namely the Arapaho, Isabelle, and Arikaree, into their head cirques; these bodies of ice are only a few tens of meters thick. In the LGM, and in many glacials before that, the glaciers fully occupied valley heads scooped into the range crest (Figs. 3 and 5). The advances and retreats of these glaciers paced the delivery of sediment to the High Plains in the major streams. The timing of the LGM and penultimate glacial advances has been established by ^{10}Be concentrations in morainal boulders near Nederland (Schildgen, 2000; Schildgen et al., 2002). The timing of retreat of glaciers in Green Lakes valley and in Fourth of July valley has been established using ^{10}Be concentrations in glacially polished rock knobs (Ward et al., 2009; Dühnforth and Anderson, 2011). This history in Green Lakes valley records a detachment of the glaciers from their morainal belts by 18 ka, stalling of retreat ca. 14 ka, and rapid final deglaciation that was completed prior to 12 ka.

Gordon Gulch (Figs. 5, 14) lies beyond the glacial limit, however, and so has evolved in the absence of direct influence

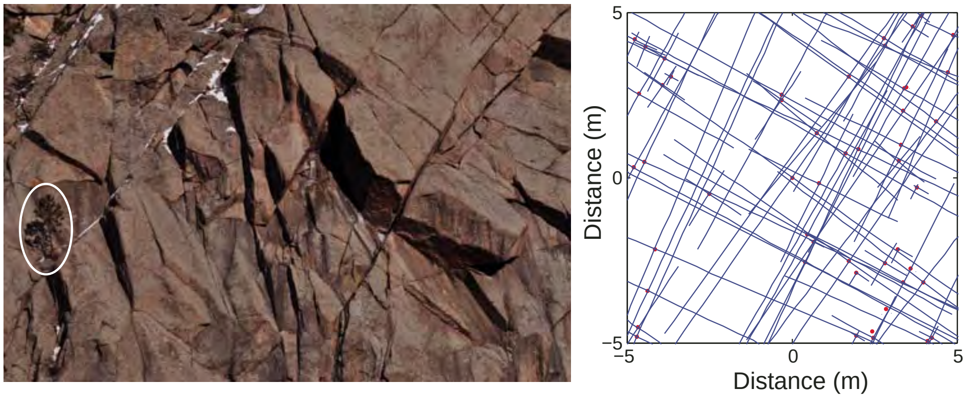

Figure 12. Left: Fracture pattern in Boulder Creek granodiorite in outcrop, lower Boulder Canyon. Note ~20-m-tall, large Ponderosa pine (circled) for scale. Prominent fracture sets intersect to generate a range of block sizes and potential flow pathways. Right: Numerically generated, two-dimensional fracture network with two specified mean fracture orientations, and a power-law distribution of lengths around a random set of initial fracture junctions (red dots).

Figure 13. View west from upper Gordon Gulch. The Arapaho Glacier is visible between the summits of South and North Arapaho peaks on the Continental Divide. Tundra-covered Caribou ridge along the left skyline separates the North Boulder Creek headwaters (including Green Lakes valley) on the right from the Middle Boulder Creek headwaters (including Fourth of July valley) on the left. Niwot Ridge, the location of the Niwot Long Term Ecological Research (LTER) site, is the next major east-trending ridge north of this view (photo taken 2 Oct 2008 by S.P. Anderson).

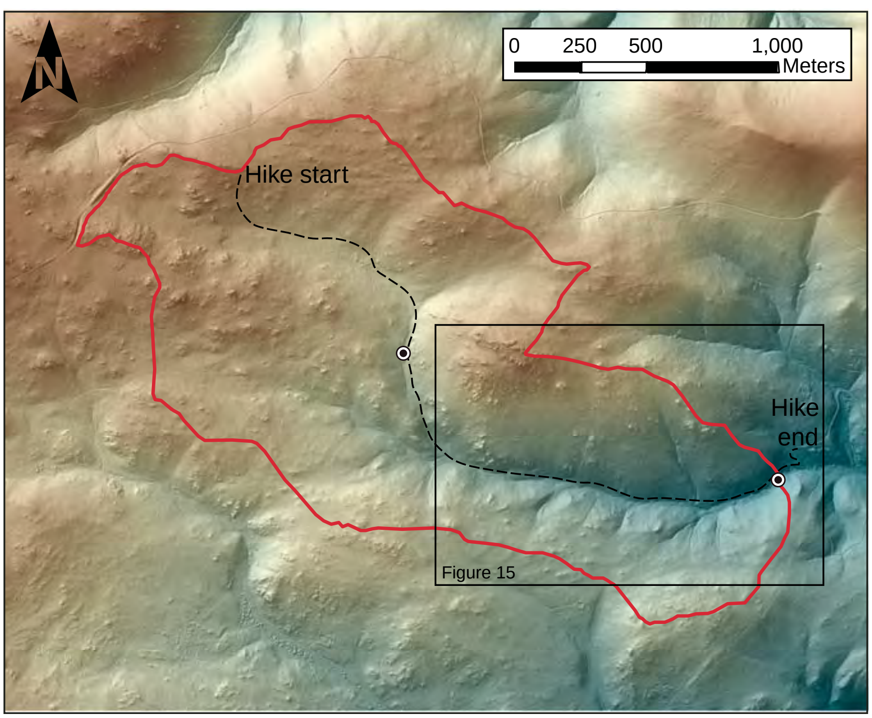

Figure 14. Gordon Gulch shaded relief map derived from bare-earth–processed light detection and ranging. Note that the landscape is dotted with rocky outcrops. Red line outlines catchment boundary above lower stream gage (circle). An upper stream gage (circle) measures stream flow from upper basin. Our hiking route shown with dashed line. Box outlines scene in Figure 15.

of glaciers. The east-west–trending watershed provides a natural experiment in which the influence of the surface energy balance imposed by differing slope aspects on critical zone development can be explored. The bedrock here is primarily early Proterozoic migmatitic sillimanite-biotite gneiss intruded by small pods of Proterozoic granites (Gable, 1996, 2000). We find differences in critical zone architecture on opposing slopes that are more than skin deep (S.P. Anderson et al., 2010, 2011). Contrasts in vegetation and snow cover on the north-facing and south-facing hillslopes are striking and obvious, even to the casual observer (Fig. 15). North-facing slopes are dominated by Lodgepole pine (*Pinus contorta*); south-facing slopes are dominated by open stands of Ponderosa pine (*Pinus ponderosa*), with much wider swaths of meadow. The tree cover and slope-related differences in incoming solar radiation generate great differences in the delivery of snowmelt to the subsurface, and in the ground surface temperature histories. Seismic refraction profiling (Fig. 16) revealed that weathered rock is ~8–14 m in thickness, and extends up to 2 m deeper on north-facing slopes than on south-facing slopes (Befus et al., 2011). The geophysical transects imply that differences in weathering and erosion rates have persisted for ~100 thousand years, based on local cosmogenic-radionuclide denudation rates (Dethier and Lazarus, 2006; Shea et al., 2012; Foster et al., 2012). The present critical zone architecture therefore contains a legacy of processes that have operated during Quaternary climate cycles (Leopold et al., 2013).

Although the depth to fresh rock varies systematically with slope aspect (Fig. 16), the character of weathering on the two slopes displays only subtle differences. Measurement of rock strength shows that rock in tors and rock beneath mobile regolith is significantly more weathered (weaker) on north-facing slopes than on south-facing slopes, although differences in chemical analyses were insignificant (Kelly et al., 2011; Kelly, 2012). Mobile regolith is slightly thinner on south-facing slopes than north-facing slopes, and there is a downslope thickening evident on steeper slopes (Shea et al., 2012; Shea, 2013). Microbial community diversity correlates with soil pH and C:N, which themselves are structured by slope aspect (Eilers, 2011). Microbial communities showed greater diversity with depth in soil profiles than across slope aspects and vegetation communities (Eilers et al., 2012). Organic matter leached from the same profiles yielded complementary findings (Gabor and McKnight, 2011). In fact, these two studies show that the variability that is so obvious at the surface (as reflected in the macroflora in Fig. 15) is much less apparent at depth in the mobile regolith. However, the organic matter becomes increasingly microbial in origin with depth, and the humic material in the upper saprolite sampled appears to be used as an electron shuttle by microbes involved in bedrock weathering (Gabor and McKnight, 2011).

The variations in thickness of the critical zone (defined here as depth to unweathered rock) on opposing slopes are produced over timespans of ~10^5 years and require contrasting conditions at depths of more than 10 m. Hillslope hydrology is strongly modulated by surface energy balance, and is affected by contrasting conditions on different slope aspects that persist through climate cycles. We therefore turn our attention to water and its movement in the subsurface as a cause of the spatial patterns in critical zone architecture. The annual hydrograph shows a

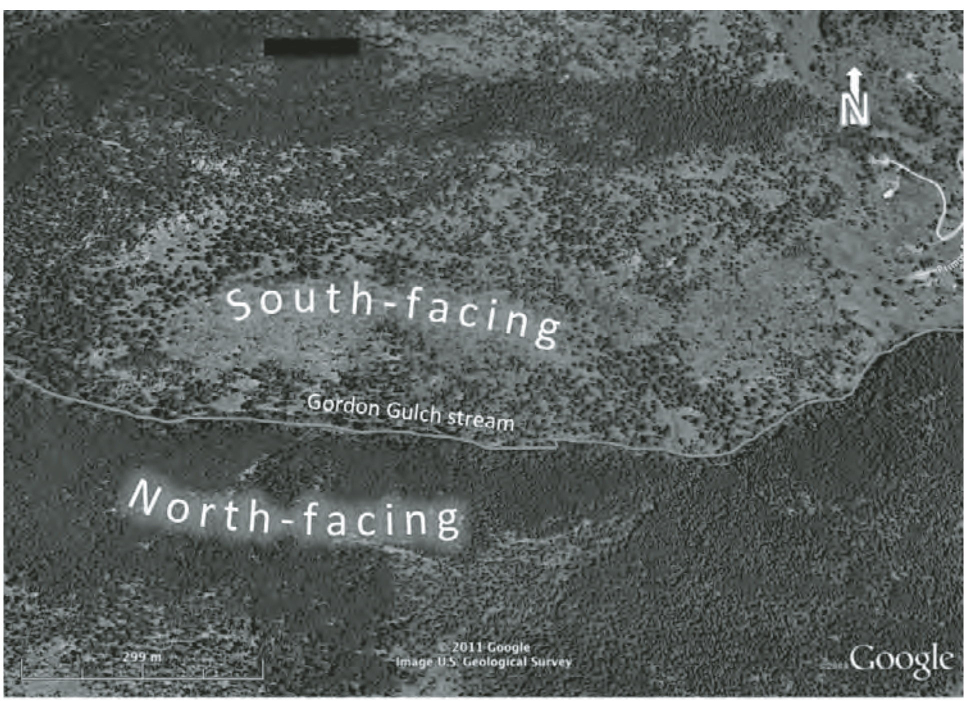

Figure 15. Google Earth image of lower Gordon Gulch, in which dense Lodgepole pine stands contrast with open Ponderosa pine woodlands on north- and south-facing slopes, respectively. Slope aspect control of vegetation in the Front Range is described by Peet (1981).

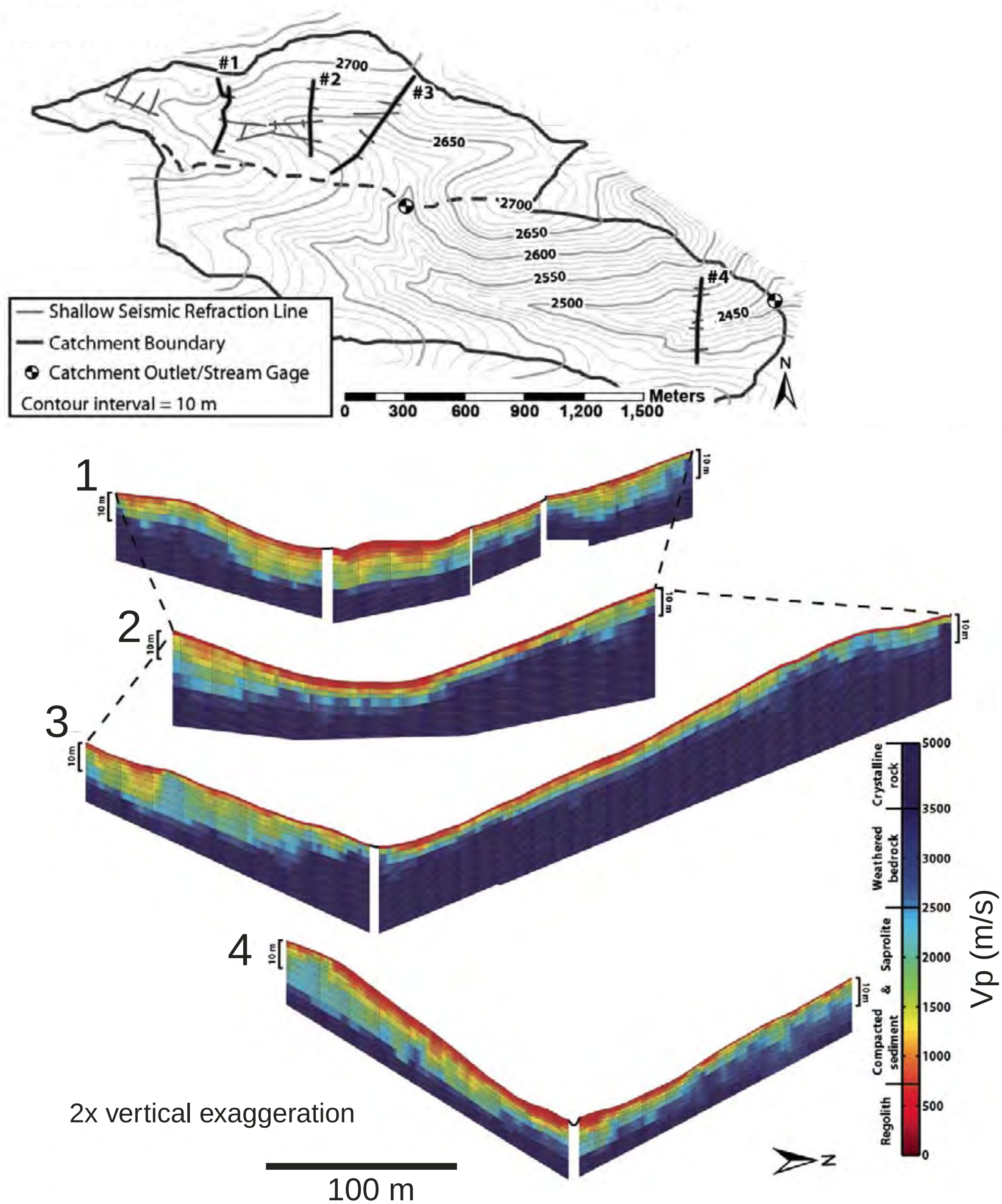

Figure 16. Shallow seismic-refraction velocity profiles in Gordon Gulch. In profile lines, north-facing slopes are on the left side, and south-facing slopes are on the right side (modified from Befus et al., 2011).

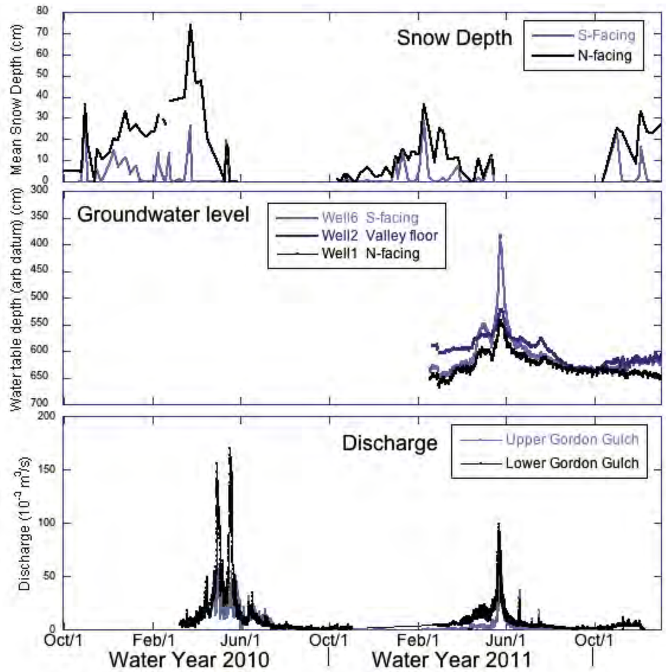

Figure 17. Snow depth, water level in three wells, and discharge at two gages in Gordon Gulch during water years 2010 and 2011. Snow depths are weekly mean values from ten manually read snowpoles on north- and south-facing slopes. Wells were installed in January 2011, and water levels here are shown relative to an arbitrary datum to show the magnitude and timing of response.

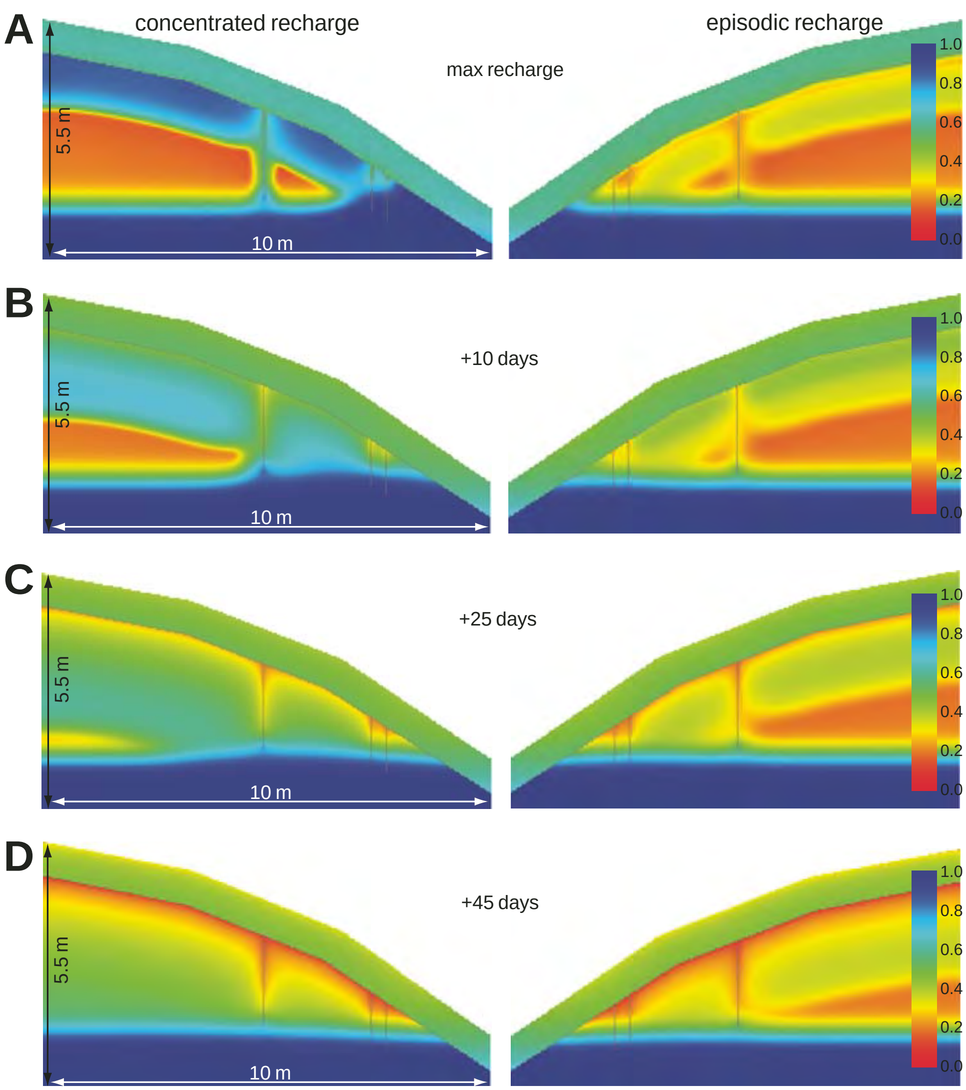

Figure 18. VS2DI model calculations of soil moisture on the lower portion of two hillslopes, comparing cases with a single, sustained recharge event (representing spring melt of the full snowpack) and several smaller recharge events (representing intermittent melting of storm snows). Upper layer represents soil, and lower material represents saprolite. Total recharge is the same in both cases. The water table was formed in the lower 1.5 m of saprolite and remained saturated during the entire model period. (A) Last day of recharge in the model year. (B) Ten days after the last recharge event. (C) Twenty-five days after the last recharge event. (D) Forty-five days after the last recharge event (from A.L. Langston, 2013, personal commun.).

snowmelt-dominated system, with peak discharge and peak water table height generally corresponding to the timing of loss of the snowpack on north-facing slopes (Fig. 17). As the sandy soils have very high infiltration rates, all water that does not evaporate enters the subsurface. This region is on the margins of the areas that develop a seasonal snowpack in the Front Range: a snowpack is sustained on north-facing slopes but is transient on south-facing slopes. Tracer experiments (Hinckley et al., 2012) revealed rapid delivery of water through soil during snow melt on north-facing slopes, while water movement on south-facing slopes was episodic, and was dominated by preferential flow. Calculations with VS2DI, a two-dimensional numerical model of vadose-zone dynamics, imply that aspect-controlled differences in the timing of snowmelt alone, independent of any variation in evapotranspiration (ET), are sufficient to account for the surprisingly strong contrast in soil moisture between the opposing slopes (Fig. 18). The differences in snow-pack evolution on north- and south-facing slopes (Jepsen et al., 2012) would therefore be expected to produce greater water delivery to underlying rock on north-facing slopes where sustained input of water during melt of an accumulated snowpack is possible (Langston et al., 2011). The conceptual model emerging (Fig. 19) is that water flux downward through variably saturated mobile regolith is controlled by delivery rate and duration, and losses through evapotranspiration, all of which vary greatly with slope aspect. At times of rapid delivery of water, relatively impermeable rock diverts water laterally. Fractures dominate the deep flow system, and the low effective porosity of this system allows large swings in the depth to groundwater, as seen in preliminary well data from Betasso.

Several lines of evidence point to differing rates of sediment transport and sediment residence time on north- versus south-facing slopes. Analysis of clay and iron accumulation rates on stable sites in the Colorado Front Range provides a basis to assess residence time for mobile regolith in Gordon Gulch catenas (Wyshnytzky and McCarthy, 2011; Dethier et al., 2012). We have also explored the use of both in situ and meteoric ^{10}Be in the Gordon Gulch catenas (Fig. 20).

In situ and meteoric ^{10}Be analyses yield steady-state lowering rates that range between 45 mm/yr (N-facing) and 30 mm/yr (S-facing) in Gordon Gulch. In addition, mobile regolith residence times on the north-facing slope (16 ka) appear to be slightly higher than those on the south-facing slope (15 ka) (Wyshnytzky and McCarthy, 2011; Shea et al., 2012; Shea, 2013; Foster et al., 2012). These conform well with the average residence times derived from iron and clay contents at the same sites (Dethier et al., 2012).

The thermal state of the landscape strongly governs the rates of physical weathering by frost cracking, and of downslope transport of mobile regolith. Modern mean annual ground surface temperatures in Gordon Gulch are only a few degrees above 0 °C.

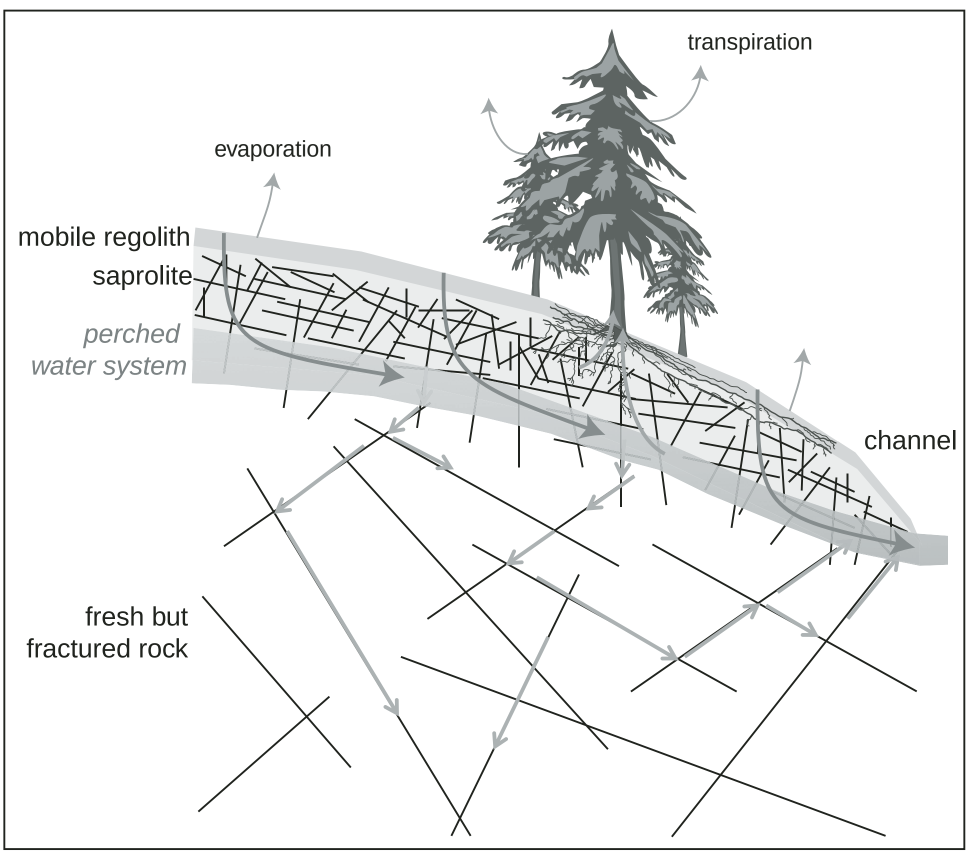

Figure 19. Conceptual picture of water flowpaths, illustrating importance of a perched water system above relatively impermeable bedrock. The deep system is dominated by flow in fractures.

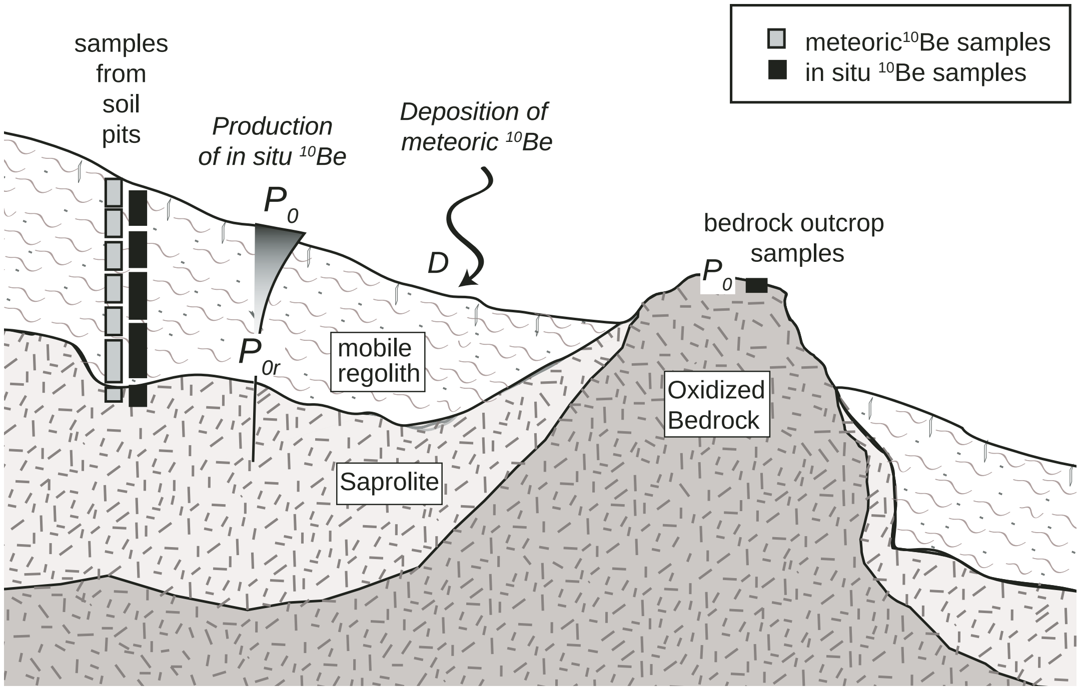

Figure 20. Schematic of sampling scheme for in situ and meteoric ^{10}Be samples in Gordon Gulch. Soil pits allow sampling for iron and clay contents as well as ^{10}Be. In situ production decays with depth, while meteoric ^{10}Be arrived in deposition on the surface. In situ samples include bedrock from beneath the soil pit and on rocky outcrops (after M. Foster, 2013, personal commun.).

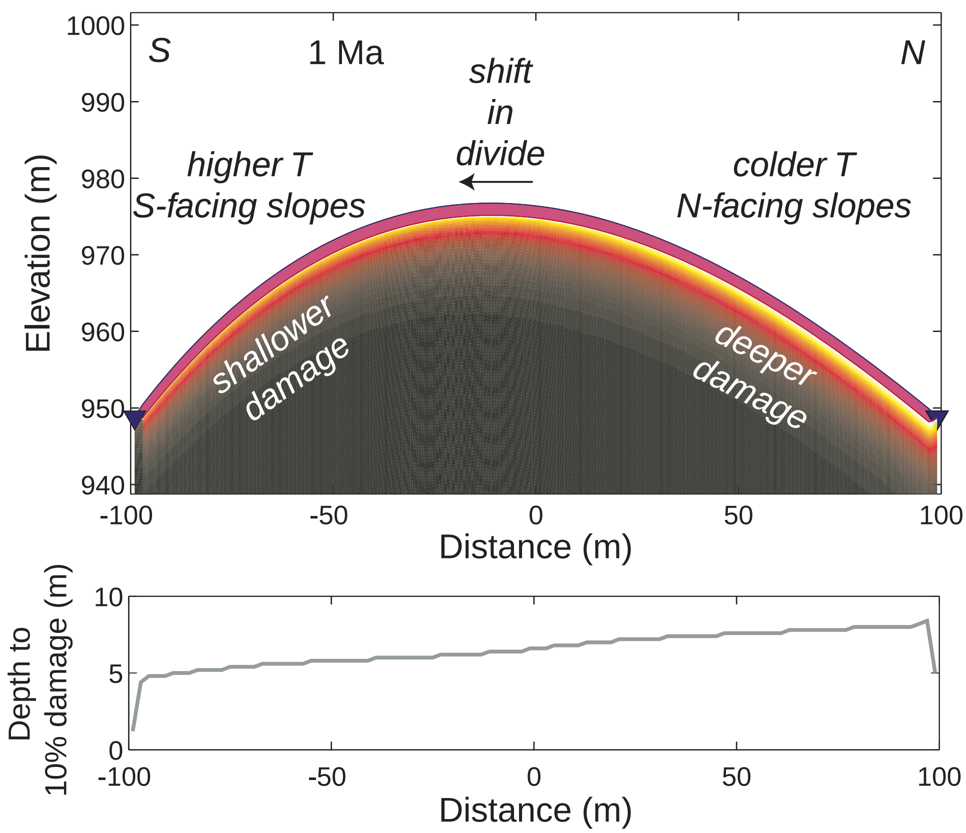

Figure 21. Results from a climate-modulated, hillslope evolution model with weathering by frost cracking and transport by frost creep after a 1 Ma model run with variable climate. The depth to the weathering front, characterized as "10% damage," is greater on the north-facing slope than on the south-facing slope, and the south-facing slope has steepened (from R.S. Anderson et al., 2012).

Because LGM conditions were likely 4–7 °C colder (e.g., Dühnforth and Anderson, 2011), it is likely that frost-related processes of variable strength have dominated the geomorphic system here over the Quaternary. R.S. Anderson et al. (2012) put forward a climate-driven model of weathering and sediment transport in which they attempt to reproduce the critical zone structure and erosion rate differences described above. The model focuses on frost cracking as a climate-modulated weathering process and frost creep as a climate-controlled transport process. Because frost-related transport rates are slower on warmer south-facing slopes, steeper slopes evolve to drive the mobile regolith transport required to balance soil production by frost cracking. The interfluve—the divide between channels—in the model therefore evolves toward an asymmetrical profile in which the divide migrates toward the south-facing slope (Fig. 21). In addition, the frost damage is shallower on the warmer south-facing slope, yielding a shallower damage zone, in accord with seismically sensed depth to fresh rock.

Elements of reality observed on slopes of both Gordon Gulch and Betasso catchments that are not captured in this model include the prominence of rocky outcrops (see Fig. 14) and the associated spatial variation in soil thickness (Shea et al., 2012; Shea, 2013). In Gordon Gulch, these reflect in part the heterogeneity of the Precambrian bedrock (interfingering of Boulder Creek granodiorite and schists), and in part variations in the fracture density.

Key Points at Stop 3

- The importance of hillslope aspect is readily apparent in the contrasting macro vegetation and snow cover on the north- and south-facing slopes.
- Microbial communities and organic matter characteristics vary with slope aspect; they vary more strongly with depth, and point to a microbial role in rock weathering.
- Shallow seismic refraction surveys show that weathered rocks extend 8–14 m below the surface and that the depth to fresh rock is greater on north-facing slopes.
- Erosion rates measured by a variety of cosmogenic techniques are 20–45 mm/yr, and the average residence time for mobile regolith is 10–20 ka.
- Although the catchment is on the margins of the seasonal snowpack, its hydrology is dominated by snowmelt and/or late spring storms.
- North-facing slopes build a seasonal snowpack, and transfer water rapidly and deeply into the subsurface during snow melt. South-facing slopes lose snow cover repeatedly in winter, and are dominated by brief preferential flow events. Hence there is less water flux into rock on south-facing slopes.
- Because the modern mean annual temperatures in Gordon Gulch are only slightly above 0 °C, it is likely that frost-related (periglacial) processes have dominated weathering and mobile regolith transport over the Quaternary.

ACKNOWLEDGMENTS

We thank Kamini Singha and Will Ouimet for careful reviews, and send kudos to Lon Abbott and Greg Hancock for their editing. The Boulder Creek Critical Zone Observatory, funded by National Science Foundation grants EAR 0724960 and 1239281, supported this work. We thank Eric Parrish, Nate Rock and Colin Millar and the entire field crew for assistance with the work.

REFERENCES CITED

Anderson, R.S., Riihimaki, C.A., Safran, E.B., and MacGregor, K.R., 2006, Facing reality: Late Cenozoic evolution of smooth peaks, glacially ornamented valleys and deep river gorges of Colorado's Front Range, *in* Willett, S.D., Hovius, N., Brandon, M.T., and Fisher, D.M., eds., Tectonics, Climate and Landscape Evolution: Geological Society of America Special Paper 398, p. 397–418.

Anderson, R.S., Anderson, S.P., and Tucker, G.E., 2012, Rock damage and regolith transport by frost: An example of climate modulation of critical zone geomorphology: Earth Surface Processes and Landforms, doi:10.1002/esp3330 (published online 18 Oct 2012).

Anderson, S.P., Bales, R.C., and Duffy, C.J., 2008, Critical Zone Observatories: Building a network to advance interdisciplinary study of Earth surface processes: Mineralogical Magazine, v. 72, no. 1, p. 7–10, doi:10.1180/minmag.2008.072.1.7.

Anderson, S.P., Blum, A.E., Hinckley, E.S., Lee, J., Gilbert, R., Trotta, J., and Dethier, D., 2010, Slope aspect and weathering in the Colorado Front Range: Geochimica et Cosmochimica Acta Supplement, v. 74, no. 12, p. A21.

Anderson, S.P., Anderson, R.S., Hinckley, E.S., Kelly, P., and Blum, A., 2011, Exploring weathering and regolith transport controls on Critical Zone development with models and natural experiments: Applied Geochemistry, v. 26, p. S3–S5, doi:10.1016/j.apgeochem.2011.03.014.

Anderson, S.P., Anderson, R.S., and Tucker, G.E., 2012, Landscape scale linkages in critical zone evolution: Comptes Rendus Geoscience, v. 344, p. 586–596, doi:10.1016/j.crte.2012.10.008.

Befus, K.M., Sheehan, A.F., Leopold, M., Anderson, S.P., and Anderson, R.S., 2011, Seismic constraints on critical zone architecture, Boulder Creek Watershed, Colorado: Vadose Zone Journal, v. 10, p. 915–927, doi:10.2136/vzj2010.0108.

Bird, P., 1988, Formation of the Rocky Mountains, Western United States: A continuum computer model: Science, v. 239, no. 4847, p. 1501–1507, doi:10.1126/science.239.4847.1501.

Bird, P., 1998, Kinematic history of the Laramide orogeny in latitudes 35°–49°N, western United States: Tectonics, v. 17, no. 5, p. 780–801.

Cole, J.C., and Braddock, W.A., 2009, Geologic map of the Estes Park 30′ × 60′ quadrangle, north-central Colorado: U.S. Geological Survey Scientific Investigations Map 3039.

Courtright, T., and Braddock, W., 1989, Geologic Map of the Table Mountain Quadrangle and Adjacent Parts of the Round Butte and Buckeye Quadrangles, Larimer County, Colorado, and Laramie County, Wyoming: U.S. Geological Survey Miscellaneous Investigations Series Map I-1805, scale 1:24,000.

Dethier, D.P., and Bove, D.J., 2011, Mineralogic and geochemical changes from alteration of granitic rocks, Boulder Creek catchment, Colorado: Vadose Zone Journal, v. 10, p. 858–866, doi:10.2136/vzj2010.0106.

Dethier, D.P., and Lazarus, E., 2006, Geomorphic inferences from regolith thickness, chemical denudation and CRN erosion rates near the glacial limit, Boulder Creek catchment and vicinity, Colorado: Geomorphology, v. 75, p. 384–399, doi:10.1016/j.geomorph.2005.07.029.

Dethier, D.P., Birkeland, P.W., and McCarthy, J.A., 2012, Using the accumulation of CBD-extractable iron and clay content to estimate soil age on stable surfaces and nearby slopes, Front Range, Colorado: Geomorphology, v. 173–174, p. 17–29, doi:10.1016/j.geomorph.2012.05.022.

Dickinson, W., Klute, M., Hayes, M., Janecke, S., Lun-din, E., McKittrick, M., and Olivares, M., 1988, Paleogeographic and paleotectonic setting of Laramide sedimentary basins in the central Rocky Mountain region: Geological Society of America Bulletin, v. 100, no. 7, p. 1023, doi:10.1130/0016-7606(1988)100<1023:PAPSOL>2.3.CO;2.

Dühnforth, M., and Anderson, R.S., 2011, Reconstructing the glacial history of Green Lakes Valley, North Boulder Creek, Colorado Front Range: Arctic, Antarctic, and Alpine Research, v. 43, no. 4, p. 527–542, doi:10.1657/1938-4246-43.4.527.

Dühnforth, M., Anderson, R.S., Ward, D.J., and Blum, A.E., 2012, Unsteady late Pleistocene incision of streams bounding the Colorado Front Range from measurements of meteoric and in situ ^{10}Be: Journal of Geophysical Research, v. 117, F01023, 20 p., doi:10.1029/2011JF002232.

Eilers, K.G., 2011, Landscape-scale variation in soil microbial communities across a forested watershed [M.A. thesis]: Boulder, University of Colorado, 44 p.

Eilers, K.G., Debenport, S., Anderson, S.P., and Fierer, N., 2012, Digging deeper to find unique microbial communities: The strong effect of depth on the structure of bacterial and archaeal communities: Soil Biology & Biochemistry, v. 50, p. 58–65, doi:10.1016/j.soilbio.2012.03.011.

Foster, M.A., Anderson, R.S., Spitzmiller, B.L., 2012, Evaluating the steady-state assumption for mobile regolith on hillslopes using in situ produced ^{10}Be, Boulder Creek CZO, Colorado Front Range, Eos (Transactions, American Geophysical Union), v. 93, no. 52, Fall Meeting Supplement, Abstract EP43E-05.

Gable, D.J., 1980, The Boulder Creek batholith, Front Range, Colorado: U.S. Geological Survey Professional Paper 1101.

Gable, D.J., 1996, Mineralogy, geochemistry, metamorphism, and provenance of the early Proterozoic metamorphic rocks of the central Front Range, Colorado: U.S. Geological Survey Open-File Report 96-522.

Gable, D.J., 2000, Geologic map of the Proterozoic rocks of the central Front Range, Colorado: U.S. Geological Survey Geologic Investigations Series I-2605, scale 1:100,000.

Gabor, R.S., and McKnight, D.M., 2011, Redox character of soil humic material suggests a role in microbial weathering of bedrock surfaces: American Chemical Society, Abstracts of Papers of the 242nd National Meeting of the American Chemical Society, Denver, Colorado, 28 August–1 September 2011, GEOC 84.

Hancock, G.S., and Anderson, R.S., 2002, Numerical modeling of fluvial terrace formation in response to oscillating climate: Geological Society of America Bulletin, v. 114, no. 9, p. 1131–1142, doi:10.1130/0016-7606(2002)114<1131:NMOFST>2.0.CO;2.

Hinckley, E.-L., Ebel, B.A., Barnes, R.T., Anderson, R.S., Williams, M.W., and Anderson, S.P., 2012, Aspect control of water movement on hillslopes near the rain-snow transition of the Colorado Front Range, U.S.A: Hydrological Processes, doi:10.1002/hyp.9549 (published online).

Jepsen, S.M., Molotch, N.P., Williams, M.W., Rittger, K.E., and Sickman, J.O., 2012, Interannual variability of snowmelt in the Sierra Nevada and Rocky Mountains, USA: Examples from two alpine watersheds: Water Resources Research, v. 48, p. W02529, doi:10.1029/2011WR011006.

Kelly, P.J., 2012, Subsurface evolution: Characterizing the physical and geochemical changes in weathered bedrock of lower Gordon Gulch, Boulder Creek Critical Zone Observatory [M.A. thesis]: Boulder, University of Colorado, 108 p.

Kelly, P.J., Anderson, S.P., Anderson, R.S., Blum, A., Foster, M., Langston, A., 2011, Subsurface Evolution: Weathering and mechanical strength reduction in bedrock of lower Gordon Gulch, Colorado Front Range: Eos (Transactions, American Geophysical Union), v. 92, no. 52, Fall Meeting Supplement, Abstract EP43C-0713.

Langston, A.L., Tucker, G.E., Anderson, R.S., and Anderson, S.P., 2011, Exploring links between vadose zone hydrology and chemical weathering in the Boulder Creek Critical Zone Observatory: Applied Geochemistry, v. 26, no. S1, p. S70–S71, doi:10.1016/j.apgeochem.2011.03.033.

Leopold, M., Völkel, J., Huber, J., and Dethier, D., 2013, Subsurface architecture of the Boulder Creek Critical Zone Observatory from electrical resistivity tomography: Earth Surface Processes and Landforms, doi:10.1002/esp.3420 (published online).

Madole, R.F., 1991, Quaternary geology of the northern Great Plains: Colorado Piedmont section, *in* Morrison, R.B., ed., Quaternary Nonglacial Geology: Conterminous U.S.: Boulder, Colorado, Geological Society of America, Geology of North America, v. K-2, p. 456–462.

Madole, R.F., Van Sistine, D.P., and Michael, J.A., 1998, Pleistocene glaciation in the upper Platte River drainage basin, Colorado: U.S. Geological Survey Scientific Investigations Map 2644, scale 1:500,000.

Mudd, S.M., and Furbish, D.J., 2007, Responses of soil-mantled hillslopes to transient channel incision rates: Journal of Geophysical Research, v. 112, p. F03S18, doi:10.1029/2006JF000516.

Muhs, D.R., and Benedict, J.B., 2006, Eolian additions to late Quaternary alpine soils, Indian Peaks Wilderness area, Colorado Front Range: Arctic, Antarctic, and Alpine Research, v. 38, no. 1, p. 120–130, doi:10.1657/1523-0430(2006)038[0120:EATLQA]2.0.CO;2.

Peet, R.K., 1981, Forest vegetation of the Colorado Front Range: Composition and dynamics: Vegetation, v. 45, p. 3–75, doi:10.1007/BF00240202.

Pepin, N., and Losleben, M., 2002, Climate change in the Colorado Rocky Mountains: Free air versus surface temperature trends: International Journal of Climatology, v. 22, p. 311–329, doi:10.1002/joc.740.

Raynolds, R., 2002, Upper Cretaceous and Tertiary stratigraphy of the Denver basin, Colorado: Rocky Mountain Geology, v. 37, no. 2, p. 111.

Riihimaki, C.A., Anderson, R.S., Safran, E.B., Dethier, D.P., and Finkel, R., 2006, Longevity and progressive abandonment of the Rocky Flats surface, Front Range, Colorado: Geomorphology, v. 78, p. 265–278, doi:10.1016/j.geomorph.2006.01.035.

Schildgen, T., 2000, Fire and Ice: Geomorphic History of Middle Boulder Creek as Determined by Isotopic Dating Techniques, Colorado Front Range [B.S. thesis]: Williamstown, Massachusetts, Williams College.

Schildgen, T.F., Dethier, D.P., Bierman, P., and Caffee, M., 2002, ^{26}Al and ^{10}Be dating of late Pleistocene and Holocene fill terraces: A record of glacial and non-glacial fluvial deposition and incision, Colorado Front Range: Earth Surface Processes and Landforms, v. 27, p. 773–787, doi:10.1002/esp.352.

Scott, G.R., 1960, Subdivision of the Quaternary Alluvium east of the Front Range near Denver, Colorado: Geological Society of America Bulletin, v. 71, p. 1541–1544, doi:10.1130/0016-7606(1960)10[1541:SOTQAE]2.0.CO;2.

Scott, G.R., 1962, Geology of the Littleton Quadrangle, Jefferson, Douglas, and Arapahoe Counties, Colorado: U.S. Geological Survey Bulletin 1121-L, 53 p.

Scott, G.R., 1963, Quaternary geology and geomorphic history of the Kassler Quadrangle, Colorado: U.S. Geological Survey Professional Paper 421-A, 70 p.

Shea, N., 2013, Spatial patterns of mobile regolith thickness and meteoric ^{10}Be in Gordon Gulch, Front Range, Colorado [M.S. thesis]: Storrs, University of Connecticut.

Shea, N., Ouimet, W., Dethier, D., Bierman, P., and Rood, D., 2012, Spatial patterns of mobile regolith thickness and meteoric ^{10}Be in the Boulder Creek Critical Zone Observatory, Front Range, Colorado: Eos (Transactions, American Geophysical Union), v. 93, no. 52, Fall Meeting Supplement, Abstract EP41D-0835.

Środoń, J., Drits, V.A., McCarty, D.K., Hsieh, J.C.C., and Eberl, D.D., 2001, Quantitative X-ray diffraction analysis of clay-bearing rocks from random preparations: Clays and Clay Minerals, v. 49, p. 514–528, doi:10.1346/CCMN.2001.0490604.

Tucker, G.E., and van der Beek, P., 2012, A simple model for post-orogenic decay of a range and its basin: Basin Research, v. 12, p. 1–19, doi:10.1111/j.1365-2117.2012.00559.x.

Ward, D.W., Anderson, R.S., Briner, J.P., and Guido, Z.S., 2009, Numerical modeling of cosmogenic deglaciation records Front Range and San Juan mountains, Colorado: Journal of Geophysical Research–Earth Surface, v. 114, F01026, doi:10.1029/2008JF001057.

Wobus, C.W., Tucker, G.E., and Anderson, R.S., 2010, Does climate change create distinctive patterns of landscape incision?: Journal of Geophysical Research, v. 115, F04008, 12 p., doi:10.1029/2009JF01562.

Wyshnytzky, C., and McCarthy, J., 2011, Meteoric ^{10}Be, fed, and clay in critical zone soils, Front Range, Colorado: Geological Society of America Abstracts with Programs, v. 43, no. 5, p. 284.

Manuscript Accepted by the Society 27 June 2013

Printed in the USA